Chin. J. Astron. Astrophys. Vol. 8 (2008), No. 5, 537–546
(*http://www.chjaa.org*)

Chinese Journal of
Astronomy and
Astrophysics

Feedback of Active Galactic Nuclei in Seyfert 2 Galaxies *

En-Peng Zhang[1], Wei-Hao Bian[2,3], Chen Hu[1], Wei-Ming Mao[1], A-Li Luo[1] and Yong-Heng Zhao[1]

[1] National Astronomical Observatory, Chinese Academy of Sciences, Beijing 100012, China; *zhangep@ihep.ac.cn*
[2] Department of Physics and Institute of Theoretical Physics, Nanjing Normal University, Nanjing 210097, China
[3] Institute of High Energy Physics, Chinese Academy of Sciences, Beijing 100049, China

Received 2007 November 12; accepted 2008 March 20

Abstract It is well accepted that feedback from active galactic nuclei (AGNs) plays an important role in the coevolution of the supermassive black hole (SMBH) and its host galaxy, but the concrete mechanism of feedback remains unclear. A considerable body of evidence suggests that AGN feedback suppresses star formation in the host galaxy. We assemble a sample of Seyfert 2 galaxies with recent observational data of compact nuclear starbursts and estimate the gas surface density as a function of column density to illuminate the relation between feedback and AGN properties. Although there are some uncertainties, our data still imply the deviation from the star formation law (Kennicutt-Schmidt law). Further, they indicate that: (1) Feedback correlates with the Eddington ratio, rather than with the mass of SMBH, as a result of decreasing star formation efficiency. (2) The SMBH and the torus are probably undergoing coevolution. Conclusions presented here can be refined through future high resolution CO or HCN observations.

Key words: galaxies: active — galaxies: Seyfert — feedback

1 INTRODUCTION

The discovery of the Supermassive black hole (SMBH) mass vs. bulge mass ($M_{\rm SMBH}$-$M_{\rm bulge}$) and $M_{\rm SMBH}$ vs. stellar velocity dispersion ($M_{\rm SMBH}$-σ) relations suggests that the evolution of the SMBH and the host galaxy are tightly coupled (Magorrian et al. 1998; Ferrarese & Merritt 2000; Gebhardt et al. 2000; Tremaine et al. 2002; Bian & Zhao 2003). Considerable effort has been made in recent years to disentangle the origin of these relations and it is now generally believed that AGN feedback plays an important role in regulating the coevolution (Silk & Rees 1998; Di Matteo et al. 2005; Croton et al. 2006; Schawinski et al. 2006). The precise nature and mechanism for this feedback remains, however, in need of further study both theoretically and observationally.

The relation between SMBH activity and the star formation rate (SFR) of the host galaxy has also been the subject of many studies in recent years in an effort to understand the mechanism by which AGN feedback operates. Energy released by accretion on to the SMBH can either trigger star formation, by dynamically compressing the gas, or suppress star formation, by blowing away the gas (Ho 2005b). Using [O II] as a tracer of SF, Ho (2005a) inferred that the SFR is much lower in a sample of PG quasars than in starburst and normal galaxies of the same range of gas content. Ho (2005a) attributed the suppression to the AGN activity, however the [O II] extinction of $A_V = 1$ in the star formation region introduces large uncertainties in this conclusion (Schweitzer et al. 2006). More recently, Shi et al. (2007) observed the 7.7

* Supported by the National Natural Science Foundation of China.

and 11.3 μm aromatic features in a sample of PG, 2MASS and 3CR AGNs including those in Ho (2005a). They found that the aromatic-based star-forming infrared (SFIR) luminosity of PG quasars, as a function of gas mass, follows that of normal galaxies. Kaviraj et al. (2007) found that, for "post-starburst" E+A galaxies with galaxy masses of $> 10^{10} M_{\odot}$, the star formation quenching efficiency increases as the galaxy mass increases. They suggested that feedback from the AGN dominates over that from the supernovae and becomes increasingly so with increasing galaxy mass. In a sample of early-type galaxies, Schawinski et al. (2007) identified an evolutionary sequence from star-forming via nuclear activity to quiescence. During this process, the star formation is suppressed by nuclear activity.

Feedback from the AGN is expected to have a stronger impact on the nuclear region than on either the bulge or the outer regions of the host galaxy. For a sample of Seyfert galaxies, Wang et al. (2007) estimated the surface density of gas ($\Sigma_{\rm gas}$) using a Kepler disk model and compared it with the star formation rates (SFRs) in compact nuclear regions (CNRs), gotten by polycyclic aromatic hydrocarbon (PAH) observations. For this sample, the SFRs are suppressed in comparison with the Kennicutt-Schmidt (K-S) law (Kennicutt 1998a). While AGN feedback is suggested as the origin of this suppression, but the relation between the properties of the AGN and the feedback efficiency remain unclear.

In this paper, we estimate the gas surface density using the neutral hydrogen column density ($N_{\rm H}$) for a sample of Seyfert 2 galaxies (S2s) and attempt to relate the deviation from the K-S law to the dimensionless AGN accretion rate (Eddington fraction) as it is an indicator of AGN activity. Our suggestions are, that the Eddington fraction rather than the SMBH mass is the key factor for understanding the AGN feedback and that the SMBH and torus are probably undergoing coevolution as a consequence of AGN feedback.

2 SAMPLE AND RESULTS

2.1 Sample and Gas Surface Density

The sample analysed in Wang et al. (2007) consists of 57 Seyfert galaxies (37 S2s & 20 S1s) with well constrained CNR SFRs (Imanishi 2002; Imanishi 2003; Imanishi & Wada 2004). The Seyfert galaxies are taken from CfA (Huchra & Burg 1992) and 12 μm sample (Rush et al. 1993). The sample is not biased either for, or against, the presence of compact nuclear starbursts (Imanishi 2003).

We use the 3.3 μm PAH emission to trace the SFR because it is intrinsically bright and not strongly affected by broad silicate dust absorption (Imanishi 2002; Wang et al. 2007). The observed 3.3 μm PAH emission originates primarily in starburst regions, associated with the dusty torus (Imanishi 2003; Imanishi & Alonson-Herrero 2004).

In a galaxy the $\Sigma_{\rm gas}$ can be traced either through CO or HCN observations, but there are no such observations for the CNRs in our sample. Instead, Wang et al. (2007) estimated $\Sigma_{\rm gas}$ using a Keplerian rotating disk model. As the compact nuclear starburst originates primarily from the torus, the physical scale is 100 pc rather than Kpc, where more powerful circumnuclear starbursts occur. For Seyfert 2 galaxies, the mass of the torus can be estimated from the absorbing column density measured from the X-ray spectra (Risaliti et al. 1999). The gas surface density in the same region is then given by:

$$\Sigma_{\rm gas} = 1.13 \times 10^4 \mathcal{C} \left(\frac{N_{\rm H}}{10^{24}\ {\rm cm}^{-2}} \right) \left(\frac{M_{\odot}}{{\rm pc}^2} \right), \quad (1)$$

where $\mathcal{C} = \cos(\theta)$ is the covering factor of the torus, and θ is the half open angle (Fig. 3). Here we neglect the difference between the torus area and its projection due to the inclination, assuming that it is geometrically thick. Even for the geometrically thin case the uncertainty is less than a factor of 2 on average, because most Seyferts have inclinations $i < 60^{\circ}$ and we can assume that the torus and the galaxy disc are co-planar (see next paragraph and Fig. 3, $A_{\rm project} = \pi r_{\rm out}^2 \cos(i)$, $r_{\rm out} \gg r_{\rm in}$). From the relative number of S1s and S2s, we obtain $\mathcal{C} \sim 0.8$. For Compton-thick objects ($N_{\rm H} > 10^{24}\ {\rm cm}^{-2}$), $\mathcal{C} \sim 0.4$ (Risaliti et al. 1999). Objects with a lower limit of $\sim 10^{24}\ {\rm cm}^{-2}$ are put into the $10^{24}\,{\rm cm}^{-2} < N_{\rm H} < 10^{25}\,{\rm cm}^{-2}$ bin (Risaliti et al. 1999). Figure 1 shows the histogram of log $N_{\rm H}$. About $\frac{2}{3}$ of the sample are heavily obscured sources ($N_{\rm H} > 10^{23}\ {\rm cm}^{-2}$).

As the geometry and distribution of the material in the torus are not well known (Haas et al. 2003), the measurement of $N_{\rm H}$ strongly depends on our viewing angle of the torus. The X-rays emitted by the central engine may also be obscured by the galaxy disk when the inclination is large. We account for this either by

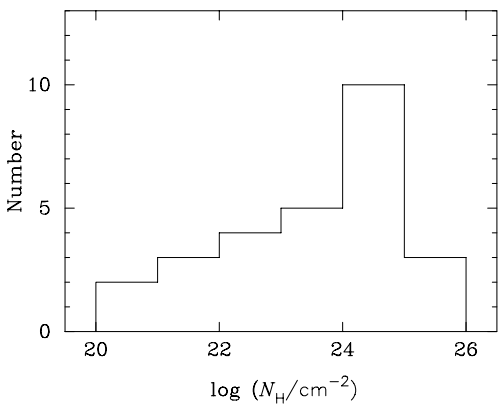

Fig. 1 Distribution of the column density ($N_{\rm H}$).

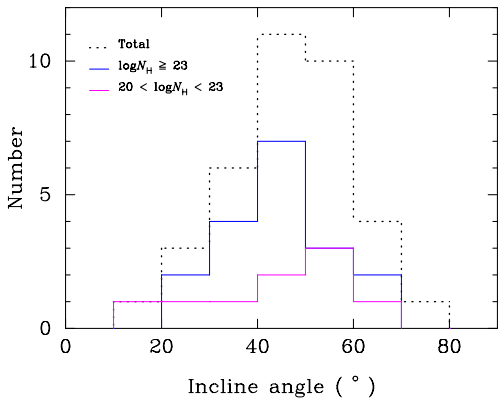

Fig. 2 Frequency distribution of the inclination angle of the galaxy disk.

finding a value for the inclination angle from the literature or by deriving it from $\sin^2 i = [1-(b/a)^2]/0.96$, where b/a is the axial ratio and a is the semi-major axis. Figure 2 shows the number distribution of i. Axial ratios lower than 0.2 are difficult to detect because of the thickness of galaxy disk. We take $b/a = 0.2$ ($i \approx 70°$) as the critical axial ratio for edge-on galaxies (Hubble 1926). For nearly all of the S2s in the sample, X-ray obscuration due to the galaxy disk can be neglected.

Determining the inclination angle of the torus remains a challenging problem. Figure 3 shows the possible position and geometry of the torus under the assumption that the torus and galaxy disk are co-planar. If the inclination of the torus changes between sources, this will affect the observed project area of the torus, which we can neglect under the assumption that the torus is geometrically thick.

S2s with $N_{\rm H} < 10^{23}$ cm^{-2} are primarily composed of intermediate Seyfert galaxies (e.g. type 1.8–1.9). Their average $N_{\rm H}$ is much lower than the "strict" Seyfert 2 with $N_{\rm H} \geq 10^{23}$ cm^{-2} (Risaliti et al. 1999). The intermediate AGN classification may be the result of lines of sight just intercepting the edge of the torus. Recently, it has been suggested that unabsorbed S2s ($N_{\rm H} < 10^{22}$ cm^{-2}) may also be a new class of objects (Panessa & Bassani 2002; Gallo et al. 2006). Unabsorbed non-hidden broad line region S2s may be the final state of the Seyfert scenario and are likely to have a significantly different gas to dust ratio compared with other AGN (Zhang & Wang 2006; Wang & Zhang 2007). To obtain the mass and the surface density of the gas more precisely, we consider the 18 "strict" S2s in our sample, whose $N_{\rm H}$ values are less strongly affected by the viewing angle.

Finally, we note that obscuration of the hard X-rays by the bulge can also be neglected, as demonstrated by the X-ray spectra of S1s taken in the context of the Unified Model of AGN (Antonucci 1993). Thus the $\Sigma_{\rm gas}$ derived here is associated with the star formation in CNRs (Imanishi 2003).

We compare our result of $\Sigma_{\rm gas}$ with the prediction of the model presented in Wang et al. (2007) in Figure 4. Sources with $N_{\rm H} \geq 10^{25}$ cm^{-2} agree well with the model. The remaining sources fall below the the model predictions. Both of these results will be tested more rigorously with more detailed observations in the future.

The method described here is unfortunately not viable for Seyfert 1 sources, but according to the Unified Model, S1s and S2s are intrinsically the same, with only a different viewing angle (Antonucci 1993) being responsible for their differing appearances. There is no appreciable difference between the CNR SFRs for S1s and S2s (Imanishi & Wada 2004), however, and thus we infer that the conclusions drawn from S2s should also be valid for S1s.

2.2 SFR, Black Hole Mass and Eddington Fraction

We convert the PAH emission into IR luminosity via $L_{\rm IR} = 10^3 L_{\rm PAH}$ with a scatter of a factor of 2–3 for pure star formation (Imanishi 2002). Wang et al. (2007) estimated the lower and upper limits of the surface

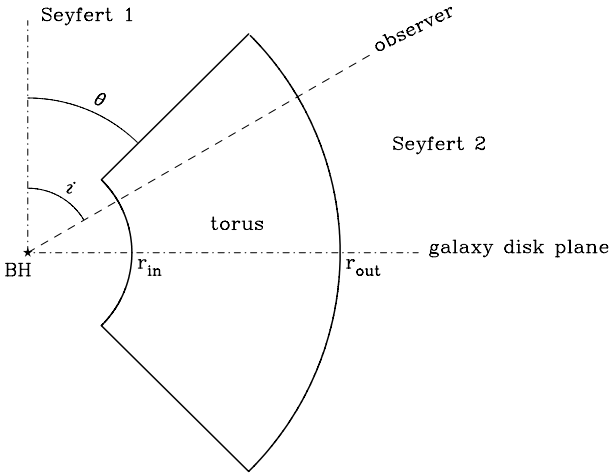

Fig. 3 Possible position and geometry of the torus. θ is the half open angle of the torus, i is the inclination angle of the galaxy disk and torus, supposed coplanar.

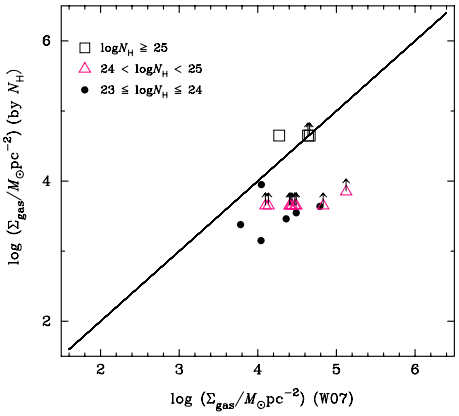

Fig. 4 Comparison of the $\Sigma_{\rm gas}$ estimated by $N_{\rm H}$ and that of Wang et al. (2007).

density of the SFRs by

$$\dot{\Sigma}^{\rm L}_{\rm SFR} = 35.8 L_{\rm PAH,41} R^{-2}_{200}\ (M_\odot\ {\rm yr}^{-1}\ {\rm kpc}^{-2}), \tag{2}$$

and

$$\dot{\Sigma}^{\rm U}_{\rm SFR} = 35.8 L_{\rm FIR,44} R^{-2}_{200}\ (M_\odot\ {\rm yr}^{-1}\ {\rm kpc}^{-2}), \tag{3}$$

respectively, where $L_{\rm PAH,41} = L_{\rm PAH}/10^{41}$ erg s^{-1} and $L_{\rm FIR,44} = L_{\rm FIR}/10^{44}$ erg s^{-1}, $L_{\rm FIR} = L_{(8-1000\mu{\rm m})}$. These equations originate from the fact that PAH grains are destroyed by EUV and X-ray photons, and that the infrared emission from Seyfert galaxies has contributions from both starburst and AGN components (Wang et al. 2007). We also take the surface density of the star formation rates as the geometric average of the two: $\dot{\Sigma}_{\rm SFR} = \left(\dot{\Sigma}^{\rm L}_{\rm SFR}\dot{\Sigma}^{\rm U}_{\rm SFR}\right)^{1/2}$. The error bars correspond to $\dot{\Sigma}^{\rm L}_{\rm SFR}$ and $\dot{\Sigma}^{\rm U}_{\rm SFR}$ (Wang et al. 2007).

For S2s, we estimate the black hole mass using the relation

$$M_{\rm SMBH} = 1.35\times10^8\left(\sigma/200\,{\rm km\ s^{-1}}\right)^{4.02} M_\odot, \tag{4}$$

where σ is the stellar velocity dispersion (Tremaine et al. 2002). The velocity dispersion can be estimated by $\sigma = \mathrm{FWHM}_{[\mathrm{OIII}]}/2.35$ (Nelson & Whittle 1996). However, it has been shown in Sloan Digital Sky Survey (SDSS) sample that $\mathrm{FWHM}_{[\mathrm{OIII}]}/2.35$ overestimates the stellar velocity dispersion by a factor of 1.34 and hence the black hole masses are also overestimated (Greene & Ho 2005). We use the corrected $\sigma_* = \sigma/1.34$ to estimate the black hole masses for objects without σ measurement.

We estimate the bolometric luminosity from $L_{\mathrm{Bol}} = 3500 L_{[\mathrm{O\ III}]}$ with a mean uncertainty of 0.38 dex (Heckman et al. 2004). The [O III] fluxes are corrected for the extinction using the relation (Bassani et al. 1999),

$$F^{\mathrm{cor}}_{[\mathrm{O\ III}]} = F^{\mathrm{obs}}_{[\mathrm{O\ III}]} \left[\frac{(\mathrm{H}\alpha/\mathrm{H}\beta)_{\mathrm{obs}}}{(\mathrm{H}\alpha/\mathrm{H}\beta)_0} \right]^{2.94}, \tag{5}$$

assuming an intrinsic Balmer decrement $(\mathrm{H}\alpha/\mathrm{H}\beta)_0 = 2.9$. Then the Eddington fraction is given by $\mathcal{E} = L_{\mathrm{Bol}}/L_{\mathrm{Edd}}$, and the Eddington luminosity $L_{\mathrm{Edd}} = 1.38 \times 10^{38} (M_{\mathrm{SMBH}}/M_\odot)\ \mathrm{erg\ s^{-1}}$.

Table 1 gives the sample of S2s. The present sample is heterogeneous and incomplete and we stress that the data from the published literature are from different authors and instruments. This leads to some uncertainties, but does not affect our conclusions within the error bars. We use the Hubble constant $H_0 = 75\ \mathrm{km\ s^{-1}\ Mpc^{-1}}$ and deceleration factor $q_0 = 0.5$ throughout this paper.

2.3 Break in the Kennicutt-Schmidt Law

Wang et al. (2007) found that in regions dominated by AGN feedback, the nuclear SFR surface density ($\dot{\Sigma}_{\mathrm{SFR}}$) does not increase with the gas surface density (Σ_{gas}) which can be taken as direct evidence for the feedback suppressing the nuclear SFR. On the other hand, the AGN parameter that drives the feedback and suppression is still unknown. Here, we concentrate on the relations between the feedback and the mass of the black hole and the Eddington fraction to reveal which one is responsible for the deviation from the K-S law.

To compare with the K-S law (Kennicutt 1998a), we define a parameter $\mathcal{K}$:

$$\mathcal{K} = \frac{\dot{\Sigma}_{\mathrm{SFR}}}{\Sigma^{\gamma}_{\mathrm{gas}}}, \tag{6}$$

where $\mathcal{K} = \mathcal{K}_0 = 2.5 \times 10^{-4}$, $\gamma = \gamma_0 = 1.4$ is often referred to as the global star formation law (Kennicutt 1998b). For our objects, we fixed γ at 1.4 to obtain $\mathcal{K}$ and then compared it with $\mathcal{K}_0$. We neglect the dispersion intrinsic to the K-S law itself for the large error bar of $\dot{\Sigma}_{\mathrm{SFR}}$.

Figure 5(a) shows the relation of $\log \mathcal{E}$ and $\log \mathcal{K}$. Using ASURV (Feigelson & Nelson 1985), we obtain

$$\log \mathcal{K} = (-0.95 \pm 0.25) \log \mathcal{E} + (-4.59 \pm 0.21). \tag{7}$$

The Spearman's coefficient $\rho = -0.63$ and the null-probability $p = 98.5\%$.

Figure 5(b) shows the relation of $\log \mathcal{K}$ and $\log M_{\mathrm{SMBH}}$:

$$\log \mathcal{K} = (0.31 \pm 0.59) \log M_{\mathrm{SMBH}} + (-6.77 \pm 4.35). \tag{8}$$

The Spearman's coefficient $\rho = -0.08$ and the null-probability $p = 24.3\%$.

We note that Mrk 938 is a remnant of a wet merger (Schweizer & Seitzer 2007) and Mrk 273 is a young merger system (Yun & Scoville 1995). Their SFRs have been significantly raised. In these sources, the feedback from supernovae dominate that from the AGN, which we exclude when we analyze the correlation.

In the K-S law, $\dot{\Sigma}_{\mathrm{SFR}}$ depends only on the property of the gas, i.e., the gas surface density (Σ_{gas}). However, Figure 5(a) shows that the SFR falls below the K-S law as the Eddington fraction increases. The higher the Eddington fraction, the greater the deviation from the K-S law. When $\log \mathcal{E} > 0$, the observed points no longer overlap the K-S law predictions within their error bars. Since the Eddington fraction is an indicator of AGN activity, this probably means that the activity of the AGN is suppressing the star formation and causing the break in the K-S law. Figure 5(b) shows M_{SMBH} has no influence on the K-S law.

On the other hand, in the AGN radiation driving feedback scenario (Wang et al. 2007), there are two critical gas surface densities between which AGN feedback dominates. These can be roughly converted to critical column densities defining the range $10^{23}\ \mathrm{cm^{-2}} \leq \mathrm{N_H} \leq 10^{26}\ \mathrm{cm^{-2}}$. The present sample covers the

Table 1 Seyfert 2 Galaxies Sample. The columns are: (1) source name; (2) redshift; (3)inclination angle of the galaxy disk (in degrees); (4) column density (in cm^{-2}); (5) stellar velocity dispersion σ (in km s^{-1}); (6) luminosity of [O III] λ5007Å (in erg s^{-1}); (7) respective references for columns (3), (4), (5) and (6); (8) black hole mass (in $M_{\odot}$); (9) the scale of the starburst regions (in kpc); (10) and (11) are the lower ($\dot{\Sigma}^{\mathrm{L}}_{\mathrm{SFR}}$) and upper ($\dot{\Sigma}^{\mathrm{U}}_{\mathrm{SFR}}$) limits of surface density of star formation rates, respectively (in $M_{\odot}$ yr^{-1} kpc^{-2}).

Object (1)	z (2)	$i(^{\circ})$ (3)	N_{H} (4)	σ (5)	$\log L_{[\mathrm{O\ III}]}$ (6)	Ref. (7)	$\log M_{\mathrm{BH}}$ (8)	R (9)	$\log \dot{\Sigma}^{\mathrm{L}}_{\mathrm{SFR}}$ (10)	$\log \dot{\Sigma}^{\mathrm{U}}_{\mathrm{SFR}}$ (11)
F01475–0740	0.017	36.3	21.59	...	41.69	1,11, 13	7.55[c]	0.26	0.66	0.99
F04385–0828	0.015	58.0	...	907[b]	40.97	1, 15,15	8.77	0.22	0.74	1.51
F15480–0344	0.030	27.6	> 24.20	664[b]	42.95	1,11, 15,13	8.22	0.43	0.66	1.37
IC3639	0.011	34.0	> 25.00	95	42.11	2,12, 17,13	6.83	0.13	1.02	2.21
MCG–3-34-64	0.017	46.8	23.60	155	41.82	1,11, 12,13	7.69	0.24	0.66	1.87
Mrk 34	0.050	57.0	> 24.00	530[b]	41.55	2,11, 2,21	7.80	0.17	0.94	1.20
Mrk 78	0.037	60.8	...	201	41.98	3, 18,17	8.14	0.41	0.97	1.37
Mrk 273	0.038	54.1	23.69	211	42.39	3,16, 17,16	8.22	0.42	1.54	2.66
Mrk 334	0.022	41.6	20.64	250[b]	41.29	4,11, 4,13	6.52	0.19	1.39	2.19
Mrk 463E	0.051	57.1	23.51	545[b]	41.90	3,11, 2,21	7.88	0.56	0.88	1.67
Mrk 477	0.038	43.2	> 24.00	473[b]	42.08	4,11, 20,21	7.63	0.42	1.10	1.49
Mrk 573	0.017	31.2	> 24.00	147	41.73	1,11, 17,21	7.58	0.24	0.66	1.16
Mrk 938	0.019	45.4	> 24.00	330[b]	42.69	4,11, 4,13	7.00	0.28	1.72	2.28
Mrk 993	0.015	46.1	...	392[b]	40.87	5, 9, 4	7.30	0.22	0.44	0.82
NGC 262	0.015	20.4	23.20	118	41.20	1,11, 18,15	7.21	0.22	1.04	1.19
NGC 513	0.020	...	...	152	40.59	18,15	7.65	0.30	0.57	1.47
NGC 1068[a]	0.004	40.0	> 25.00	140	42.12	25,11, 17,19	6.90	0.15	1.95	2.23
NGC 1194	0.013	53.6	...	396[b]	40.45	1, 10,23	7.32	0.19	0.57	0.85
NGC 1241	0.014	53.6	...	136	41.74	4, 17,24	7.46	0.18	0.27	1.92
NGC 1320	0.010	71.0	...	116	40.93	2, 18,21	7.18	0.15	0.92	1.44
NGC 1667	0.015	38.0	> 24.00	149	41.16	2,11, 19,19	7.62	0.19	0.44	2.10
NGC 2992	0.008	62.0	21.84	172	40.42	2,11, 19,19	7.87	0.12	1.09	2.00
NGC 3660	0.012	43.2	> 20.26	95	40.88	6,11, 19,19	6.83	0.19	0.66	1.43
NGC 3786	0.009	58.0	...	142	41.52	2, 18, 4	7.53	0.13	0.92	1.30
NGC 4388	0.008	60.1	23.43	111	40.54	1,11, 19,19	7.10	0.12	0.66	2.12
NGC 4501	0.008	59.7	> 21.03	151	39.90	7,11, 15,14	7.64	0.12	0.66	2.43
NGC 4968	0.010	66.0	> 24.00	121	41.64	2,16, 19,19	7.25	0.15	1.04	1.45
NGC 5135	0.014	48.2	24.00	143	40.95	4,14, 19,19	7.54	0.16	1.52	2.59
NGC 5252	0.023	54.1	22.64	209	41.96	5,13, 19,13	8.21	0.33	0.87	1.30
NGC 5256	0.028	41.6	25.00	315[b]	41.82	8,14, 14,13	6.92	0.31	1.30	2.23
NGC 5347	0.008	38.2	> 24.00	93	41.22	1,11, 18,24	6.79	0.12	0.92	1.31
NGC 5674	0.025	23.5	22.85	129	40.85	9,16, 17,19	7.36	0.21	0.80	1.87
NGC 5695	0.014	41.6	...	144	40.86	9, 18,14	7.56	0.18	0.44	1.14
NGC 5929	0.008	18.0	22.63	119	40.87	2,11, 17,14	7.22	0.12	0.27	2.09
NGC 7172	0.009	56.0	22.95	154	40.84	10,11, 17,24	7.67	0.10	1.06	2.16
NGC 7674	0.029	43.2	> 24.00	144	42.08	1,11, 18,15	7.56	0.42	1.04	1.88
NGC 7682	0.017	36.0	...	152	41.14	2, 19,19	7.65	0.24	0.44	0.76

Notes: [a] NGC1068 M_{BH} is taken from Lodato & Bertin (2003); Star formation rate is taken from Davies et al. (2007). [b] refers to [O III] FWHM. [c] based on $M_{\mathrm{BH}} - M_{\mathrm{bulge}}$ relation, F01475-0740: $M_{\mathrm{bulge}} = -18.80$.

References: (1) Schmitt et al. (2001); (2) Whittle (1992); (3) Keel (1980); (4) Dahari & Robertis (1988); (5) Malkan (1998); (6) Gerhardt et al. (2006); (7) Jarrett et al. (2003); (8) Hunt & Malkan (2004); (9) De Robertis et al. (1998); (10) Schmitt et al. (1997); (11) Shu et al. (2007); (12) Lumsden et al. (2001); (13) Gu & Huang (2002); (14) Tran (2003); (15) Wang & Zhang (2007); (16) Bassani (1999); (17) Garcia-Rissmann et al.(2005); (18) Nelson & Whittle (1995); (19) Gu et al. (2006); (20) De Robertis & Shaw (1990); (21) Cid Fernandes et al. (2001); (22) Panessa et al. (2006); (23) de Grijp et al. (1992); (24) Zhang & Wang (2006); (25) Davies et al. (2007).

transition state from starburst-powered to AGN-powered (Wang et al. 2007). Figure 5(a) shows that some objects with $N_{\mathrm{H}} \leq 10^{24}\ \mathrm{cm}^{-2}$ obey the K-S law as AGN activity begins to dominate the starburst.

The deviation from the global SF law may mean that the star formation efficiency (SFE) is, itself, altered by AGN feedback. The SFE can be investigated through the star formation efficiency per unit dynamical time, defined as $\mathcal{F} = \frac{\dot{\Sigma}_{\mathrm{SFR}}\tau_{\mathrm{dyn}}}{\Sigma_{\mathrm{gas}}}$, where τ_{dyn} is the dynamical time scale (Silk 1997; Kennicutt 1998b).

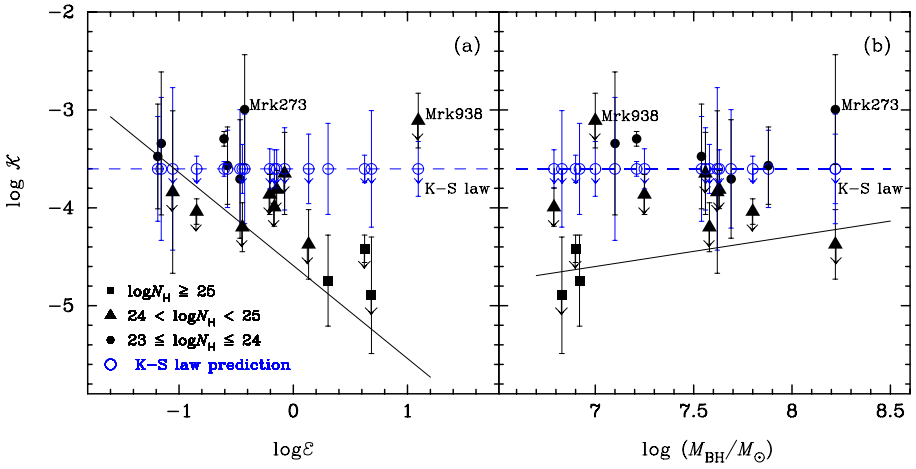

Fig. 5 K-S law and mass and Eddington fraction of black hole. The black symbols are derived from the observed values and the black line is the fitting. The open circles are the prediction of the K-S law ($\dot{\Sigma}_{\rm SFR} = 2.5 \times 10^{-4}\Sigma_{\rm gas}^{1.4}$,). The error bars refer to the black symbols. The blue dashed line is not a fit: it just marks the value $\log(2.5 \times 10^{-4})$.

Young et al. (1986) used the ratio of SFR to the molecular gas mass as the SFE, i.e.,

$$\mathrm{SFE} = \frac{\dot{\Sigma}_{\rm SFR}}{\Sigma_{\rm gas}} \,. \tag{9}$$

Using ASURV, we obtain

$$\log \mathrm{SFE} = (-0.35 \pm 0.12) \log \mathcal{E} + (-0.33 \pm 0.09) \,. \tag{10}$$

The Spearman coefficient $\rho = -0.46$ and the null-probability $p = 92.2\%$. Also,

$$\log \mathrm{SFE} = (0.30 \pm 0.27) \log M_{\rm SMBH} + (-2.33 \pm 2.03) \,. \tag{11}$$

The Spearman coefficient $\rho = -0.086$ and the null-probability $p = 26.2\%$.

The foregoing equations show, the higher the Eddington fraction, the lower the SFE. Since a lower SFE means a higher feedback efficiency, this demonstrates that the Eddington fraction, rather than the SMBH mass, is the key factor in understanding the AGN feedback. The break of the SF law is caused by the lower SFE due to AGN feedback. Imanishi (2002) showed that more powerful AGNs have more powerful compact starbursts. Figure 5(a) shows that the higher the obscuring column density, the higher the Eddington fraction. If more powerful AGNs have a greater reservoir of fueling gas, then the associated starburst will be powerful because the gas density is high, although it dose not mean the SFE is high.

2.4 Possible Coevolution of Black Hole and Torus

We have shown that AGN feedback has important impact on the SF of the CNR. The evolution of the SMBH and the CNR (torus) should couple together. Neglecting the accretion onto the black hole ($\sim 10^{-2} \sim 10^{-3}$ of the SFR of the gas - see Fig. 6), the SFR of the CNR can be taken to be the growth rate of the torus.

Figure 6 shows the relation of the accretion rate of SMBHs and the SFRs of the CNRs. We find

$$\log \mathrm{SFR} = (0.49 \pm 0.10) \log \dot{M}_{\rm acc} + (1.72 \pm 0.11) \,, \tag{12}$$

where $\mathrm{SFR} = \pi R^2 \dot{\Sigma}_{\rm SFR}$, R is scale of the CNR. The physical accretion rate of SMBH is $\dot{M}_{\rm acc} = L_{\rm bol}/\eta c^2$ and $\eta = 0.1$ is the accretion efficiency. The Spearman coefficient $\rho = 0.62$ and the null-probability $p =$

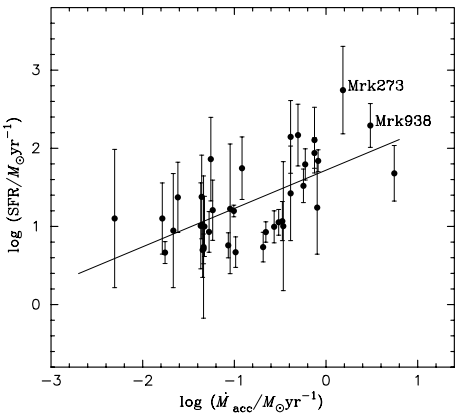

Fig. 6 Cogrowth of the CNRs and the black holes.

99.99%. Here, we include all the S2s because, according to the Unified Model, these results should be appropriate for all Seyfert galaxies. We have pointed out that Mrk 273 and Mrk 938 are merger system which central engines have, by AGN standards, just been triggered and thus the main energy source is the starburst. These sources represent the initial stage of coevolution of SMBH and CNR, so they are also included when we analyze the correlation here.

It has been found that the coevolution of BH and host spheroid can be a consequence of the feedback (Hao et al. 2008). Figure 6 shows the co-evolution of the SMBH and the compact nuclear environment (torus). We suggest that this is a consequence of AGN feedback.

3 CONCLUSIONS AND DISCUSSION

Using the $N_{\rm H}$ to estimate $\Sigma_{\rm gas}$ for a small sample of nearby Seyfert 2 galaxies, we investigated the relation between AGN feedback and the SF of the host galaxy CNRs. Though there are large uncertainties in the estimation of $\Sigma_{\rm gas}$, our data nevertheless imply deviation from the star formation law (K-S law). Further, it seems (1) that the feedback efficiency is correlated with the Eddington fraction rather than with the SMBH mass (The higher Eddington fraction, the higher the feedback efficiency); (2) that the SMBH and the torus are probably undergoing coevolution.

However, there are inevitably some uncertainties contained within these conclusions. The most important uncertainty is in the estimation of $\Sigma_{\rm gas}$. Although we only use "strict" S2s when estimating $\Sigma_{\rm gas}$, it remains uncertain as to what extent their $N_{\rm H}$ measurements are affected by the viewing angle. Determining the inclination angle, geometry and gas distribution of the torus is a challenge and so we assume that the geometry is the same as that in Nenkova et al. (2002), i.e., the distribution of the obscuring material in the torus is isotropic, and $N_{\rm H}$ is then constant in any radial direction when $i > \theta$ (see Fig. 3). The scale of the torus is also a source of uncertainty and remains widely debated in the literature. Imanishi (2003) assumed the compact nuclear starburst originates in the outer regions of the torus, and Imanishi & Alonson-Herrero (2004) have provided a quantitative test of this assumption. Risaliti et al. (1999) suggested that a Compton thin torus ($\sim 10^{23}$ cm^{-2}) can extend over 100 pc in scale while a Compton thick one is likely to be more compact. If this is the case, it is not clear how much of the torus mass is located on scales larger than what we assumed in this work. If the gas can not be detected when measuring $N_{\rm H}$, then the masses detailed here are a lower limit for the region we discussed. Further, if the gas mass can not be neglected, $\Sigma_{\rm gas}$ will increase more rapidly for Compton thick objects than for Compton thin ones. According to Equation (6), $\mathcal{K}$ will decrease more for Compton thick objects and thus our conclusions will become stronger (as can be seen from Fig. 5(a)). Here we assumed the nucleus to have a similar structure and mass distribution profile along any radial direction.

Based on S1 and S2 number counts, the covering factor of the torus is $\mathcal{C} = 0.8$. For Compton thick objects, we adjust this to 0.4, considering the extension and dynamic mass of the torus (Risaliti et al. 1999).

Wang et al. (2005) proposed a more precise method to determine $\mathcal{C}$ for PG quasars, but there is still no good way to determine the covering factor of the torus in type 2 objects. Instead, we resort to a constant geometry that is defined by source statistics. If we adopt $\mathcal{C} = 0.8$ for Compton thick objects, our conclusions will become more robust (Fig. 5(a)). Additionally, we demonstrated that because $\theta < i$ for S2s and $\mathcal{C} = \cos\theta$, the variation of $\mathcal{C}$ will be less than a factor of 2 on average as θ varies from 0° to 60°. It is plausible that the covering factor may evolve with the luminosity (Wang et al. 2005), but this is not important because the range of bolometric luminosity is small in the present sample. The uncertainties due to the covering factor can be absorbed into the upper and lower limits of the SFR but we note that the geometry of the obscuring gas is still widely debated. Solving this problem is, however, beyond the scope of the present paper. The uncertainties from estimating the bolometric luminosity and Eddington luminosity are small compared with the upper and lower limits of the $\dot{\Sigma}_{\rm SFR}$, and will not strongly effect our conclusions. Finally, the estimation of $\Sigma_{\rm gas}$ from $N_{\rm H}$ is, by its very nature, a first order approximation.

To date, there is still no consensus on the mechanisms by which feedback from AGN impacts on their host environment (Ho 2005b). Our results provide some constraints for further studies of AGN feedback and its evolution. According to the evolutionary picture of the Unified Model (Zhang & Wang 2006; Wang & Zhang 2007), when AGN are triggered (probably by mergers), their accretion rates are initially small. AGN feedback, at this stage, does not dominate over the feedback from the supernovae. The first phase of AGN activity may be revealed in optical selected narrow line Seyfert 1 galaxies (NLS1s) or type 1 QSOs (Wang & Zhang 2007). The AGN accretion rates then increase rapidly and the sources then appear as soft X-ray selected narrow line objects (indeed NLS1s show different X-ray spectra, see Williams et al. 2004 and Bian et al. 2006). At this stage the accretion rate reaches its highest point and the SMBH grows rapidly. Meanwhile, the AGN feedback efficiency is very high and the SMBH growth and host galaxy properties become tightly coupled. In the final state of AGN evolution, the accretion rate drops dramatically due to the lack of fueling gas and the feedback becomes less effective.

Our data indicate independence of SF suppression on the SMBH mass. However, Schawinski et al. (2006) found that the fraction of star-forming early-type galaxies is anti-correlated with the stellar velocity dispersion. We think the inconsiatency could be caused by (1) The range of BH mass in our sample is narrower than in theirs (in our sample $\sigma < 200\,{\rm km\ s^{-1}}$, while in Schawinski et al. (2006) σ extends to $> 300\,{\rm km\ s^{-1}}$). (2) The uncertainties of estimation of the $\Sigma_{\rm gas}$ and the SFR. Indeed, all the results presented in this paper should be refined with future high-resolution CO or HCN observations, to determine the gas properties and more precise estimation of SFR for a larger sample of AGN.

Acknowledgements E.-P. Zhang is grateful to J.-M. Wang, Y.-M. Chen and others in the AGN group at the IHEP, Beijing, for valuable discussions. We also thank the staff in the LAMOST project in NAOC for the useful discussions. We are grateful to Nick Schurch for polishing up the English. We are also grateful to the referee for comments and suggetions which are valuable to improve the paper. This research is supported by the NSFC through Nos. 60402041, 10778724 and LAMOST Project.

References

Antonucci R. R. J., 1993, ARA&A, 31, 473
Bassani L. et al., 1999, ApJS, 121, 473
Bian W.-H., Zhao Y.-H., 2003, Chin. J. Astron. Astrophys. (ChJAA), 3, 119
Bian W.-H., Cui Q.-L. Chao L.-H., 2006, Chin. J. Astron. Astrophys. (ChJAA), 6, 281
Cid Fernandes R. et al., 2001, ApJ, 558, 81
Croton D. J. et al., 2006, MNRAS, 365, 11
Dahari O., De Robertis M. M., 1988, ApJS, 67, 249
Davies R. I., Mueller S. F., Genzel R. et al., 2007, ApJ, 671, 1388
de Grijp M. H. K., Keel W. C., Miley G. K. et al., 1992, A&AS, 96, 389
De Robertis M. M., Hayhoe K., Yee H. K. C., 1998, 115, 163
De Robertis M. M., Shaw R. A., 1990, ApJ, 348, 421
Di Matteo T., Springel V., Hernquist L., 2005, Nature, 433, 604
Feigelson E. D., Nelson P. I., 1985, ApJ, 293, 192
Ferrarese L., Merritt D., 2000, ApJ, 539, L9

Gallo L. C. et al., 2006, MNRAS, 365, 688
Garcia-Rissmann A., Vega L. R., Asari N. V. et al., 2005, MNRAS, 359, 765
Gebhardt K. et al., 2000, ApJ, 539, L13
Gerhardt E. M. et al., 2006, ApJS, 165, 307
Greene J. E., Ho L. C., 2005, ApJ, 627, 721
Gu Q., Huang J., 2002, ApJ, 579, 205
Gu Q., Melnick J., Cid Fernandes R. et al., 2006, MNRAS, 366, 480
Haas M. et al., 2003, A&A, 402, 87
Heckman T. M., Kauffmann G., Brinchmann J. et al., 2004, ApJ, 613, 109
Hao C. N., Xia X. Y., Mao S., Deng Z. G. et al., 2008, Chin. J. Astron. Astrophys. (ChJAA), 8, 12
Ho L. C., 2005a, ApJ, 629, 680
Ho L. C., 2005b, astro-ph/0511571
Hubble E., 1926, ApJ, 64, 321
Huchra J., Burg R., 1992, ApJ, 393, 90
Hunt L. K., Malkan M. A., 2004, ApJ, 616, 707
Imanishi M., 2002, ApJ, 569, 44
Imanishi M., 2003, ApJ, 599, 918
Imanishi M., Alonson-Herrero A., 2004, ApJ, 614, 122
Imanishi M., Wada K., 2004, ApJ, 617, 214
Jarrett T. H., Chester T., Cutri R., Schneider S. E. et al., 2003, AJ, 125, 525
Kaviraj S., Kirkby L. A., Silk J. et al., 2007, 382, 960
Keel W. C., 1980, AJ, 85, 198
Kennicutt R. C., 1998a, ARA&A, 36, 189
Kennicutt R. C., 1998b, ApJ, 498, 541
Lodato G., Bertin G., 2003, A&A, 398, 517
Lumsden S. L., Heisler C. A., Bailey J. A. et al., 2001, MNRAS, 327, 459
Magorrian J. et al., 1998, AJ, 115, 2285
Malkan M. A., Gorjian V., Tam R., 1998, ApJS, 117, 25
Nelson C. H., Whittle M., 1996, ApJ, 465, 96
Nelson C. H., Whittle M., 1995, ApJS, 99, 67
Nenkova M., Ivezic, Z., Elitzur M., 2002, ApJ, 570, L9
Panessa F., Bassani L., 2002, A&A, 394, 435
Panessa F., Bassani L., Cappi M. et al., 2006, A&A, 455, 173
Risaliti G., Maiolino R., Salvati M., 1999, ApJ, 522, 157
Rush B., Malkan M. A., Spinoglio L., 1993, ApJS, 89, 1
Schawinski K. et al., 2006, Nature, 442, 888
Schawinski K. et al., 2007, MNRAS, 382, 1415
Schmitt H. R., Antonucci R. R. J., Ulvestad J. S. et al., 2001, ApJ, 555, 663
Schmitt H. R., Kinney A. L., Storchi-Bergmann T. et al., 1997, ApJ, 477, 623
Schweitzer M. et al., 2006, ApJ, 649, 79
Schweizer F., Seitzer P., 2007, AJ, 133, 2132
Shi Y. et al., 2007, ApJ, 669, 841
Shu X. W., Wang J. X., Jiang P. et al., 2007, ApJ, 657, 167
Silk J. 1997, ApJ, 481, 703
Silk J., Rees M. J., 1998, A&A, 331, L1
Tran H. D., 2003, ApJ, 583, 632
Tremaine S. et al., 2002, ApJ, 574, 740
Wang J.-M., Chen Y.-M., Yan C.-S. et al., 2007, ApJ, 661, L143
Wang J.-M., Zhang E.-P., Luo B., 2005, ApJ, 627, L5
Wang J.-M., Zhang E.-P., 2007, 660, 1072
Whittle M., 1992, ApJS, 79, 49
Williams R. J., Mathur S., Pogge R. W., 2004, ApJ, 610, 737
Young J. S. et al., 1986, ApJ, 311, L17
Yun M. S., Scoville N. Z., 1995, ApJ, 451, L45
Zhang E.-P., Wang J.-M., 2006, ApJ, 653, 137